Effects of finite electron temperature on gradient drift instabilities in partially magnetized plasmas

V. P. Lakhin, V. I. Ilgisonis, A. I. Smolyakov, E. A. Sorokina, and N. A. Marusov

Citation: Physics of Plasmas **25**, 012106 (2018); doi: 10.1063/1.4996708
View online: https://doi.org/10.1063/1.4996708
View Table of Contents: http://aip.scitation.org/toc/php/25/1
Published by the American Institute of Physics

Articles you may be interested in

Marginal stability, characteristic frequencies, and growth rates of gradient drift modes in partially magnetized plasmas with finite electron temperature
Physics of Plasmas **25**, 012107 (2018); 10.1063/1.4996719

Nonlinear structures and anomalous transport in partially magnetized $E \times B$ plasmas
Physics of Plasmas **25**, 011608 (2018); 10.1063/1.5001206

Current flow instability and nonlinear structures in dissipative two-fluid plasmas
Physics of Plasmas **25**, 011604 (2018); 10.1063/1.5017521

Turbulent heating due to magnetic reconnection
Physics of Plasmas **25**, 012304 (2018); 10.1063/1.4993423

Weak turbulence theory for beam-plasma interaction
Physics of Plasmas **25**, 011603 (2018); 10.1063/1.5017518

Excitation of a global plasma mode by an intense electron beam in a dc discharge
Physics of Plasmas **25**, 011606 (2018); 10.1063/1.5018427

Effects of finite electron temperature on gradient drift instabilities in partially magnetized plasmas

V. P. Lakhin,[1,2] V. I. Ilgisonis,[2,3] A. I. Smolyakov,[1,2,4] E. A. Sorokina,[1,2] and N. A. Marusov[1,2,5]

[1]*NRC "Kurchatov Institute", 1 Kurchatov Sq., Moscow, 123182, Russia*
[2]*Peoples' Friendship University of Russia (RUDN University), 3 Ordzhonikidze St., Moscow, 117198, Russia*
[3]*State Atomic Energy Corporation ROSATOM, 24 Bolshaya Ordynka St., Moscow, 119017, Russia*
[4]*University of Saskatchewan, 116 Science Place, Saskatoon, SK S7N 5E2, Canada*
[5]*Moscow Institute of Physics and Technology, 9 Institutskiy per., Dolgoprudny, 141701, Russia*

(Received 18 July 2017; accepted 25 November 2017; published online 5 January 2018)

The gradient-drift instabilities of partially magnetized plasmas in plasma devices with crossed electric and magnetic fields are investigated in the framework of the two-fluid model with finite electron temperature in an inhomogeneous magnetic field. The finite electron Larmor radius (FLR) effects are also included via the gyroviscosity tensor taking into account the magnetic field gradient. This model correctly describes the electron dynamics for $k_\perp \rho_e > 1$ in the sense of Padé approximants (here, $k_\perp$ and ρ_e are the wavenumber perpendicular to the magnetic field and the electron Larmor radius, respectively). The local dispersion relation for electrostatic plasma perturbations with the frequency in the range between the ion and electron cyclotron frequencies and propagating strictly perpendicular to the magnetic field is derived. The dispersion relation includes the effects of the equilibrium $\mathbf{E} \times \mathbf{B}$ electron current, finite ion velocity, electron inertia, electron FLR, magnetic field gradients, and Debye length effects. The necessary and sufficient condition of stability is derived, and the stability boundary is found. It is shown that, in general, the electron inertia and FLR effects stabilize the short-wavelength perturbations. In some cases, such effects completely suppress the high-frequency short-wavelength modes so that only the long-wavelength low-frequency (with respect to the lower-hybrid frequency) modes remain unstable. *Published by AIP Publishing.* https://doi.org/10.1063/1.4996708

I. INTRODUCTION

Plasmas immersed in the external magnetic field $\mathbf{B}_0$ with externally applied electric field $\mathbf{E}_0$ (perpendicular to $\mathbf{B}_0$) are subject to many instabilities.[1,2] Such instabilities with frequencies ω in the range between the ion cyclotron frequency ω_{Bi} and the electron cyclotron frequency ω_{Be}, $\omega_{Bi} \ll \omega \ll \omega_{Be}$, are of great importance to both laboratory and space plasmas. In particular, they are important for magnetron plasma discharges, Hall ion sources, Penning discharges, closed drift thrusters (Hall thrusters) (see, e.g., Refs. 3, 4 and references therein), open-mirror devices,[5–7] as well as for a variety of ionosphere and magnetosphere plasma conditions. These instabilities are thought to be the source of turbulence and anomalous transport phenomena such as electron resistivity and turbulent plasma heating.[5–8]

In situations with the moderate magnetic field with $\rho_i \gg L$ but $\rho_e \ll L$, where ρ_e and ρ_i are the electron and ion Larmor radii, respectively, L is the device length, and the considered frequency range $\omega_{Bi} \ll \omega \ll \omega_{Be}$, the influence of the magnetic field on ions is negligible while the electrons are magnetized and mainly drift perpendicular to the magnetic field. Such partially magnetized plasmas will be called Hall plasma below. The standard drift waves of fully magnetized plasmas[1] do not exist in plasmas with unmagnetized ions, but plasma density gradients result in the appearance of the so-called antidrift-mode.[9]

The externally applied electric field produces stationary $\mathbf{E}_0 \times \mathbf{B}_0$ electron drift which can result in destabilization of the anti-drift mode. Combination of the magnetic field and plasma density inhomogeneities results in a number of gradient drift instabilities in Hall plasmas.[1,2,10] In particular, such an instability has been studied in the context of the magnetic-mirror systems.[5,6,11,12] The gradient drift instability has been identified experimentally and studied theoretically[13,14] in Hall plasma thrusters, also see some recent works.[15,16] The general dispersion relation for perturbations with $k_\parallel = 0$ ($k_\parallel$ is the component of a wavevector along the equilibrium magnetic field) has been derived in Refs. 13 and 14. This dispersion relation, which is the third order in ω, has been analyzed in Refs. 13–16 only in some limiting cases under simplifying assumptions (for the discussion of the simplifications, see Ref. 17).

As discussed in Refs. 13, 14, and 17, the gradient-drift instability is traditionally thought to be responsible for high-frequency short-wavelength oscillations in Hall plasmas. In this paper, we show that electron inertia and finite Larmor radius (FLR) effects stabilize the short-wavelength modes, and for some parameters, only the low-frequency modes are excited near the instability boundaries. Therefore, gradient-drift instability can be considered as a possible mechanism of low-frequency oscillations and structure formation in experiments with Hall plasmas.[13,18] Recently, a linear theory of this instability in the long-wavelength limit has been studied in Ref. 19 with the dispersion relation similar to Refs. 13 and

14. The dispersion relation for long-wavelength perturbations has been revised in Refs. 20 and 21. The authors of these papers have taken into account the full compressibility of the electron flow for the vacuum magnetic field. They have also generalized the dispersion relation for long-wavelength modes taking into account the electron temperature inhomogeneity and its perturbations. The influence of plasma density, temperature, and magnetic field gradients on shorter-wavelength higher-frequency oscillations in the lower-hybrid frequency range has been also studied in Refs. 22–26.

In this paper, we present an analysis of stability of electrostatic plasma perturbations in the frequency range $\omega_{Bi} \ll \omega \ll \omega_{Be}$ and propagating strictly perpendicular to the magnetic field. Thus, we leave the modified two-stream instability, which requires the finite value of $k_\parallel$, out of consideration. Also, we neglect plasma ionization and electron collisions with neutrals assuming that ω exceeds the ionization and collision frequencies. The low-frequency instabilities in Hall thruster plasmas due to collisions and ionization processes have been studied in Refs. 18, 27, and 28.

We use an advanced hydrodynamic model for electrons which includes the effects of finite electron temperature and FLR including the regime $k_\perp \rho_e > 1$. Another novel feature of our model is that the magnetic field gradients are included not only in the compressibility of the lowest order electron flow (as in previous works) but also into the higher order FLR terms. The temperature inhomogeneity and its perturbation are neglected. Ions are considered to be cold. We show that the local dispersion relation can be reduced to the cubic equation in ω with a general structure similar to the dispersion relation of Refs. 12–14. We derive an explicit analytical stability criterion without making any additional assumptions concerning the wave frequencies, wavenumbers, and equilibrium plasma parameters. Based on our analysis, we predict the stabilization of the short-wavelength and high-frequency modes in some practical cases.

This paper is organized as follows. In Sec. II, we present the starting two-fluid equations, in particular, the equations of electron dynamics that take into account the finite temperature, inertia, and gyroviscosity. This model describes the electron FLR effects in Padé approximation as well as the effects of the magnetic field gradients. We also briefly discuss plasma equilibrium in the external magnetic field when the external perpendicular electric field is applied to plasma. In Sec. III, we derive the general dispersion relation for gradient drift perturbations taking into account the finite electron Larmor radius effects and discuss its consistency in various limiting cases with the dispersion relations derived earlier.[12,14,20] In Sec. IV, we present the stability analysis of gradient drift perturbations. We obtain the stability criterion in the explicit analytical form, present the stability diagram, and discuss the role of the electron inertia and FLR effects. A short summary is given in Sec. V.

II. INITIAL EQUATIONS

In this paper, we use a two-fluid model. The ions are assumed to be unmagnetized and cold. Then, the ion motion is described by the equation

$$\frac{\partial \mathbf{v}_i}{\partial t} + (\mathbf{v}_i \cdot \nabla)\mathbf{v}_i = \frac{e}{m_i}\mathbf{E}. \tag{1}$$

The ion density satisfies the continuity equation

$$\frac{\partial n_i}{\partial t} + \nabla \cdot (n_i \mathbf{v}_i) = 0. \tag{2}$$

Here, $\mathbf{v}_i$ and n_i are the ion velocity and density, $\mathbf{E}$ is the electric field, e is the proton charge, and m_i is the ion mass.

For electrons, we use the momentum equation in the following form:

$$\frac{\partial \mathbf{v}_e}{\partial t} + (\mathbf{v}_e \cdot \nabla)\mathbf{v}_e = -\frac{e}{m_e}\left(\mathbf{E} + \frac{1}{c}\mathbf{v}_e \times \mathbf{B}\right) - \frac{\nabla p_e}{m_e n_e} - \frac{\nabla \cdot \boldsymbol{\pi}_e}{m_e n_e}, \tag{3}$$

where $\mathbf{v}_e$, p_e, n_e, and $\boldsymbol{\pi}_e$ are the electron velocity, pressure, density, and gyroviscosity tensor,[1,29] c is the speed of light, and $\mathbf{B}$ is the magnetic field. The electron density is defined by the electron continuity equation

$$\frac{\partial n_e}{\partial t} + \nabla \cdot (n_e \mathbf{v}_e) = 0. \tag{4}$$

The electron temperature $T_e = p_e/n_e$ is assumed to be homogeneous, and its perturbation is neglected.

The set of Eqs. (1)–(4) is closed with the Poisson equation

$$\nabla \cdot \mathbf{E} = 4\pi e(n_i - n_e). \tag{5}$$

We consider a simplified slab model in Cartesian coordinates (x, y, z) with the z coordinate along the predominant magnetic field, the y coordinate in the periodic azimuthal direction, and the x coordinate in the direction of the applied electric field $\mathbf{E}_0 = E_0\mathbf{e}_x$ (or the direction of plasma inhomogeneity). The magnetic field is assumed to be $\mathbf{B}_0 = B_{0x}(x,z)\mathbf{e}_x + B_{0z}(x,z)\mathbf{e}_z$ and $B_{0z} \gg B_{0x}$, so that $B_0 = (B_{0x}^2 + B_{0z}^2)^{1/2} \approx |B_{0z}|$ and mainly depends on x.

Adopted for the coaxial Hall thrusters, in which the external magnetic field is assumed to be predominantly in the radial direction, the local z coordinate is in the radial direction, the x coordinate is in the axial direction, and the y coordinate is in the symmetrical azimuthal direction. The equilibrium electric field $\mathbf{E}_0 = E_0\mathbf{e}_x$ is in the axial direction. For the cylindrical magnetrons (Penning discharge configuration) with the axial magnetic field, the local z coordinate is axial, the x coordinate is radial, the y coordinate is azimuthal, and the electric field $\mathbf{E}_0$ is radial.

An explicit expression for the gyroviscosity tensor gradient $\nabla \cdot \boldsymbol{\pi}_e$ in the curvilinear inhomogeneous magnetic field can be written in the coordinate-free vector form. We start from the corresponding expression for the gyroviscosity tensor derived in Ref. 29. It follows from Eqs. (4.7), (4.14), and (4.15) of Ref. 29 that in the auxiliary Cartesian coordinate system, the gyroviscosity tensor has a form

$$\pi_{ij} = -\frac{p_e}{4\omega_{Be}}\left[(\delta_{j\nu} + 3b_j b_\nu)e_{i\gamma\mu} + (\delta_{i\nu} + 3b_i b_\nu)e_{j\gamma\mu}\right] \times b_\gamma\left(\frac{\partial v_\mu}{\partial x_\nu} + \frac{\partial v_\nu}{\partial x_\mu}\right), \tag{6}$$

where $\mathbf{b} = \mathbf{B}/B$ is the unit vector in the direction of the magnetic field, δ_{ij} is the Kronecker symbol, and e_{ijk} is the antisymmetric tensor. For simplicity, we have omitted the subscript e and mean that π_{ij} and $\mathbf{v}$ are the electron viscosity tensor and electron velocity.

Then, using the identity

$$\frac{\partial v_j}{\partial x_i} - \frac{\partial v_i}{\partial x_j} = e_{ijk}\Omega_k,$$

where $\mathbf{\Omega} = \nabla \times \mathbf{v}$, expression (6) can be represented in the form (see details of calculation in Ref. 30)

$$\pi_{ij} = -\frac{\partial}{\partial x_\mu}\left[\frac{p_e}{2\omega_{Be}}(e_{i\gamma\mu}v_j + e_{j\gamma\mu}v_i)b_\gamma\right] + \frac{p_e}{2\omega_{Be}}(\mathbf{\Omega}\cdot\mathbf{b})\delta_{ij} - f_i v_j - f_j v_i - a_i b_j - a_j b_i.$$

Here, two new vectors $\mathbf{f}$ and $\mathbf{a}$ are defined as

$$\mathbf{f} = \nabla \times \left(\frac{p_e}{2\omega_{Be}}\mathbf{b}\right),$$
$$\mathbf{a} = \frac{p_e}{2\omega_{Be}}\left\{\mathbf{b}\times[\mathbf{b}\times\mathbf{\Omega} + 3(\mathbf{b}\cdot\nabla)\mathbf{v}] + \frac{1}{2}(\mathbf{\Omega}\cdot\mathbf{b})\mathbf{b}\right\}. \tag{7}$$

Now, directly applying a differentiation with respect to x_j, we obtain

$$\frac{\partial \pi_{ij}}{\partial x_j} = e_{i\mu\gamma}\frac{\partial}{\partial x_\mu}\left[(\mathbf{v}\cdot\nabla)\left(\frac{p_e}{2\omega_{Be}}b_\gamma\right) + \frac{p_e}{2\omega_{Be}}b_\gamma(\nabla\cdot\mathbf{v})\right] + \frac{\partial}{\partial x_i}\left(\frac{p_e}{2\omega_{Be}}(\mathbf{\Omega}\cdot\mathbf{b})\right) - f_i(\nabla\cdot\mathbf{v}) - (\mathbf{v}\cdot\nabla)f_i - (\mathbf{f}\cdot\nabla)v_i - (\mathbf{B}\cdot\nabla)\left(\frac{a_i}{B}\right) - B_i\nabla\cdot\left(\frac{\mathbf{a}}{B}\right) - \left(\frac{\mathbf{a}}{B}\cdot\nabla\right)B_i.$$

Using another identity which takes place for any vectors $\mathbf{c} = \nabla\times\mathbf{C}$ and $\mathbf{d}$,

$$c_i(\nabla\cdot\mathbf{d}) + (\mathbf{d}\cdot\nabla)c_i + (\mathbf{c}\cdot\nabla)d_i \equiv 2(\mathbf{c}\cdot\nabla)d_i + (\nabla\times(\mathbf{c}\times\mathbf{d}))_i,$$

going to the vector notation, and returning the omitted subscript e, we finally obtain

$$\nabla\cdot\boldsymbol{\pi}_e = -m_e n_e(\mathbf{U}_{\star e}\cdot\nabla)\mathbf{v}_e + \nabla\left(\frac{p_e}{2\omega_{Be}}\mathbf{b}\cdot\mathbf{\Omega}\right) - 2(\mathbf{B}\cdot\nabla)\frac{\mathbf{a}}{B} + \nabla\times\left\{\frac{p_e}{2\omega_{Be}}[2(\mathbf{b}\cdot\nabla)\mathbf{v}_e + (\nabla\cdot\mathbf{v}_e - 3\mathbf{b}(\mathbf{b}\cdot\nabla)\mathbf{v}_e)\mathbf{b}]\right\}. \tag{8}$$

Here,

$$\mathbf{U}_{\star e} = \frac{1}{m_e n_e}\nabla\times\left(\frac{p_e}{\omega_{Be}}\mathbf{b}\right). \tag{9}$$

Substituting expression (8) in the electron momentum equation (3) and taking into account Eq. (7), we arrive at the following equation:

$$m_e n_e\left(\frac{\partial}{\partial t} + (\mathbf{v}_e - \mathbf{U}_{\star e})\cdot\nabla\right)\mathbf{v}_e + \nabla\times\left\{\frac{p_e}{2\omega_{Be}}[2(\mathbf{b}\cdot\nabla)\mathbf{v}_e + (\nabla\cdot\mathbf{v}_e - 3\mathbf{b}(\mathbf{b}\cdot\nabla)\mathbf{v}_e)\mathbf{b}]\right\} = -en_e\left(\mathbf{E} + \frac{1}{c}\mathbf{v}_e\times\mathbf{B}\right) - \nabla\left(p_e + \frac{p_e}{2\omega_{Be}}\mathbf{b}\cdot\mathbf{\Omega}\right) + (\mathbf{B}\cdot\nabla)\left[\frac{p_e}{\omega_{Be}}\left\{\mathbf{b}\times[\mathbf{b}\times\mathbf{\Omega} + 3(\mathbf{b}\cdot\nabla)\mathbf{v}] + \frac{1}{2}(\mathbf{\Omega}\cdot\mathbf{b})\mathbf{b}\right\}\right]. \tag{10}$$

Further, we assume that the plasma pressure is low and neglect the perturbations of the magnetic field due to plasma currents. Then, the magnetic field is assumed to be the vacuum field created by external coils, $\nabla\times\mathbf{B}_0 = 0$. Also, we assume that the electron temperature is homogeneous, $\nabla T_e = 0$. Under the above assumptions, it follows from Eq. (9) that

$$\mathbf{U}_{\star e} = \mathbf{V}_p - \mathbf{V}_D,\ \mathbf{V}_p = \frac{cT_e}{eB_0}\nabla\ln n_e\times\mathbf{b},\ \mathbf{V}_D = \frac{2cT_e}{eB_0}\nabla\ln B_0\times\mathbf{b}. \tag{11}$$

We consider slow processes with characteristic frequency scales $\omega \ll \omega_{Be}^{-1}$. Then, Eq. (10) can be solved by an expansion in the series over ω_{Be}^{-1}. In the leading order, one has

$$\mathbf{v}_e^{(0)} = \mathbf{V}_E + \mathbf{V}_p,\ \mathbf{V}_E = \frac{c}{B_0}\mathbf{E}\times\mathbf{b}. \tag{12}$$

In the next order, we take into account the electron inertia and gyroviscosity effects. We restrict ourselves to plasma motions perpendicular to the magnetic field and also neglect any inhomogeneities along the magnetic field. Under these assumptions, it follows from Eq. (10) that

$$\mathbf{v}_e^{(1)} = \frac{1}{\omega_{Be}}\left\{\left[\frac{\partial}{\partial t} + (\mathbf{V}_E + \mathbf{V}_D)\cdot\nabla\right]\mathbf{v}_e^{(0)} + \frac{1}{m_e n_e}\nabla\times\left(\frac{p_e}{2\omega_{Be}}(\nabla\cdot\mathbf{v}_e^{(0)})\mathbf{b}\right) + \frac{1}{m_e n_e}\nabla\left(\frac{p_e}{2\omega_{Be}}\mathbf{b}\cdot(\nabla\times\mathbf{v}_e^{(0)})\right)\right\}\times\mathbf{b}. \tag{13}$$

We have taken into account Eqs. (11) and (12) to reproduce a well-known gyroviscous cancellation in the first term on the right hand side of Eq. (13). Unlike the case of the straight homogeneous magnetic field, the electron magnetic drift velocity $\mathbf{V}_D$ appears in combination with $\mathbf{E}\times\mathbf{B}_0$ electron drift, $\mathbf{V}_E$, in the convective derivative operator.

Substituting expressions (12) and (13) in the electron continuity equation (4), we obtain

$$\left(\frac{\partial}{\partial t} + \mathbf{V}_E\cdot\nabla\right)n_e - 2n_e(\mathbf{V}_E + \mathbf{V}_p)\cdot\nabla\ln B_0 + \nabla_\perp^2\left(\frac{n_e T_e}{m_e\omega_{Be}^2}(\mathbf{V}_E + \mathbf{V}_p)\cdot\nabla\ln B_0\right) - \frac{1}{m_e\omega_{Be}}\left\{\nabla\left(\frac{n_e T_e}{\omega_{Be}B_0}\nabla\cdot\left((\mathbf{V}_E + \mathbf{V}_p)\times\mathbf{B}_0\right)\right)\times\mathbf{b}\right\}\cdot\nabla\ln B_0 + \nabla\cdot\left\{\frac{n_e}{\omega_{Be}}\left[\left(\frac{\partial}{\partial t} + (\mathbf{V}_E + \mathbf{V}_D)\cdot\nabla\right)(\mathbf{V}_E + \mathbf{V}_p)\right]\times\mathbf{b}\right\} = 0. \tag{14}$$

Equations (1), (2), (5), and (14) constitute a closed set of equations which will be used below to study gradient drift modes.

The magnetized electrons drift in the y direction with the velocity

$$\mathbf{v}_{0e} = (V_{0E} + V_{\star e})\mathbf{e}_y,\ V_{0E} = -\frac{c}{B_0}E_0,\ V_{\star e} = -\frac{cT_e}{eB_0}\frac{d\ln n_{0e}}{dx},$$

where T_e and n_{0e} are the equilibrium electron temperature and density.

Under the assumption of ballistic acceleration of ions in the electric field, it follows from Eq. (1) that their velocity $\mathbf{v}_{0i} = v_{0i}(x)\mathbf{e}_x$ satisfies the condition

$$v_{0i}\frac{dv_{0i}}{dx} = \frac{e}{m_i}E_0.$$

Then, according to Eq. (2), $n_{0i}(x)v_{0i}(x) = \text{const}$, and therefore, the ion motion results in density inhomogeneity

$$\frac{1}{n_{0i}}\frac{dn_{0i}}{dx} = -\frac{1}{v_{0i}}\frac{dv_{0i}}{dx} \equiv \frac{V_{0E}\omega_{Bi}}{v_{0i}^2}, \tag{15}$$

so that the density inhomogeneity is related to the applied electric field. Plasma stability for such an equilibrium has been considered in Ref. 14. Actually, the experimental data from different Hall devices show that the assumption $n_{0i}(x)v_{0i}(x) = \text{const}$ is not satisfied for the whole plasma channel. The deviation of the equilibrium from the above described one may be related to factors such as radial divergence of ion flow, ionization processes, electron collisions with neutral atoms, and wall effects (see discussion in Ref. 21). Therefore, we will not specify the equilibrium in such a way but just will assume that in the equilibrium, ions move along the electric field with the velocity v_{0i}, electrons drift in the y direction, and plasma is inhomogeneous and quasineutral, $n_{0i} = n_{0e} = n_0$.

III. DISPERSION RELATION FOR ELECTROSTATIC PERTURBATIONS

We consider the electrostatic, $\mathbf{E}' = -\nabla\phi'$, perturbations which depend only on the perpendicular coordinates (x, y) with respect to the predominant magnetic field. We restrict ourselves to local analysis. Therefore, we assume the spatio-temporal dependence of perturbations f in the Fourier form $f \sim \exp(i\mathbf{kx} - i\omega t)$, where $\mathbf{k} = (k_x, k_y, 0)$ is the wave-vector and ω is the frequency. It is assumed that the wavelength in the x direction is small compared to typical inhomogeneity lengths L of the equilibrium density, magnetic and electric fields, $k_x L \gg 1$, and the frequency of perturbations is in the range $\omega_{Bi} \ll \omega \ll \omega_{Be}$, where $\omega_{B\alpha} = eB_0/m_\alpha c$, $\alpha = (i, e)$ are the ion and electron cyclotron frequencies. Also, it is assumed that $\omega \gg kv_{Ti}$, where $v_{Ti} = (2T_i/m_i)^{1/2}$ is the ion thermal velocity, and therefore, the cold ion approximation is justified.

We represent the ion velocity and density as $\mathbf{v}_i = v_{0i}\mathbf{e}_x + \mathbf{v}_i'$, $n_i = n_0 + n_i'$, where $\mathbf{v}_i', n_i'$ are small perturbations of ion velocity and density such that $(|\mathbf{v}_i'|, n_i') \ll (v_{0i}, n_0)$. Then, linearizing Eqs. (1) and (2) with respect to perturbations, we obtain

$$(\omega - k_x v_{0i})\mathbf{v}_i' = \frac{e\mathbf{k}}{m_i}\phi',\ \ (\omega - k_x v_{0i})n_i' - n_0(\mathbf{k}\mathbf{v}_i') = 0. \tag{16}$$

Equations (16) give the following expression for the ion density perturbation:

$$n_i' = \frac{ek_\perp^2 n_0}{m_i(\omega - k_x v_{0i})^2}\phi', \tag{17}$$

where $k_\perp^2 = k_x^2 + k_y^2$.

Linearizing Eq. (14) with respect to small-scale perturbations, we obtain

$$\left[\omega - \omega_E - \omega_D + k_\perp^2\rho_e^2(\omega - \omega_E - 2\omega_D)\right]n_e' = \left[\omega_{\star e} - \omega_D + k_\perp^2\rho_e^2(\omega - \omega_E - 2\omega_D)\right]\frac{en_0}{T_e}\phi'.$$

Here, n_e' is the electron density perturbation, $\rho_e = (T_e/m_e\omega_{Be}^2)^{1/2}$ is the electron Larmor radius, and the corresponding frequencies are defined as follows:

$$\omega_E = k_y V_{0E},\quad \omega_{\star e} = k_y V_{\star e},\quad \omega_D = k_y V_D,$$

where $V_D = -(2cT_e/eB_0)d\ln B_0/dx$ is the electron magnetic drift velocity.

Then, the perturbed electron density can be written as

$$n_e' = \frac{1}{1 + k_\perp^2\rho_e^2}\left[\frac{\omega_{\star e} - \bar{\omega}_D}{\omega - \omega_E - \bar{\omega}_D} + k_\perp^2\rho_e^2\right]\frac{en_0}{T_e}\phi', \tag{18}$$

where

$$\bar{\omega}_D = \frac{1 + 2k_\perp^2\rho_e^2}{1 + k_\perp^2\rho_e^2}\cdot\omega_D.$$

For long-wavelength perturbations, $k_\perp^2\rho_e^2 \ll 1$, Eq. (18) reduces to the expression given by Eq. (16) of Ref. 20 as follows:

$$n_e' = \frac{en_0}{T_e}\cdot\frac{\omega_{\star e} - \omega_D}{\omega - \omega_E - \omega_D}\phi'.$$

In the limit of finite but small $k_\perp^2\rho_e^2$, Eq. (18) is the asymptotically exact approximation for the perturbed electron density as compared to the kinetic expressions. In the short-wavelength limit $k_\perp^2\rho_e^2 \gg 1$, the electron density perturbation in Eq. (18) reduces to the Boltzmann form $n_e' = (en_0/T_e)\phi'$ as also follows from the kinetic theory. Therefore, Eq. (18) corresponds to the Padé approximation for the perturbed electron density providing qualitatively correct description of the perturbed density in the intermediate range of wavelengths $k_\perp^2\rho_e^2 > 1$.[31]

Substituting expressions for the ion and electron density perturbations (17) and (18) in the perturbed Poisson equation $k_\perp^2\phi' = 4\pi e(n_i' - n_e')$, we finally arrive at the dispersion relation

$$1+\frac{\omega_{pe}^2}{\omega_{Be}^2}\cdot\frac{1}{1+k_\perp^2\rho_e^2}-\frac{\omega_{pi}^2}{(\omega-k_x v_{0i})^2}+\frac{1}{k_\perp^2 d_e^2}\cdot\frac{1}{1+k_\perp^2\rho_e^2}\cdot\frac{\omega_{\star e}-\bar{\omega}_D}{\omega-\omega_E-\bar{\omega}_D}=0. \tag{19}$$

Here, $d_e=(T_e/4\pi e^2 n_0)^{1/2}$ is the electron Debye radius. This dispersion relation describes both the long-wavelength modes studied earlier in Ref. 20 and short-wavelength modes with the frequencies of the order of lower-hybrid frequency, $\omega\simeq\omega_{lh}\equiv\omega_{pi}\,(1+\omega_{pe}^2/\omega_{Be}^2)^{-1/2}$. In the long-wavelength limit, it transforms into the dispersion relation derived in Ref. 20. In fact, taking a limit $k_\perp^2\rho_e^2\to 0$ and neglecting the first two terms in Eq. (19) corresponding to charge separation and electron inertia, we reduce it to the form which coincides with the dispersion relation derived in Ref. 20 as follows:

$$\frac{\omega_{\star e}-\omega_D}{\omega-\omega_E-\omega_D}-\frac{k_\perp^2 c_s^2}{(\omega-k_x v_{0i})^2}=0. \tag{20}$$

Here $c_s=(T_e/m_i)^{1/2}$ is the speed of sound. In the cold electron approximation, $T_e\to 0$, dispersion relation (19) can be written as

$$1+\frac{\omega_{pe}^2}{\omega_{Be}^2}-\frac{\omega_{pi}^2}{(\omega-k_x v_{0i})^2}-\frac{\omega_{pe}^2}{\omega_{Be}(\omega-\omega_E)}\cdot\frac{k_y(\kappa_n-2\kappa_B)}{k_\perp^2}=0, \tag{21}$$

where $\kappa_{n,B}\equiv d\ln(n_0,B_0)/dx$. Substituting in Eq. (21) κ_n corresponding to the ballistic acceleration of ions (15), one can easily show that it takes a form similar to the dispersion relation of Ref. 14 with two differences: (1) the dispersion relation of Ref. 14 takes into account the electromagnetic effects which are small for most Hall plasma devices [note, that the electromagnetic effects are important only for the long-wavelength perturbations with $k_\perp^2 c^2\lesssim\omega_{pe}^2/(1+\omega_{Be}^2/\omega_{pe}^2)$;[14] for typical parameters the electromagnetic effects cannot be neglected for the perturbations with the wavelength comparable to the device length scale]; (2) there is a difference in the terms proportional to κ_B due to an incomplete account of the electron flow compressibility in Ref. 14 (see a discussion of this matter in Ref. 20). Also, it is necessary to mention that for a straight homogeneous magnetic field, dispersion relation (21) transforms into the dispersion relation derived earlier in Refs. 1 and 12 in the context of experiments with plasmas in the magnetic mirror system.

The instability of perturbations described by dispersion relation (19) can be driven only by the equilibrium ion, v_{0i}, or electron, V_{0E}, V_D, flows perpendicular to the magnetic field (in the denominators of the third and fourth terms, respectively). Therefore, the gradient drift instabilities studied are sometimes called the instabilities driven by perpendicular current.[1] The instability driven by the ion current alone was noted in Ref. 10.

IV. STABILITY ANALYSIS

The dispersion relation obtained in Eq. (19) is cubic with respect to perturbation frequency ω, and this significantly complicates its direct analysis. We are unaware of any detailed analytical studies of this dispersion relation in general form which would allow to trace how a stability condition changes with the wavelength of perturbations. Usually, only the limiting cases of this equation are studied analytically (see, e.g., Refs. 12, 14, and 20). We will show here that this dispersion relation allows a sufficiently compact analytical criterion of stability.

For the analysis of stability, it is convenient to rewrite the dispersion relation (19) in the normalized form

$$1-\frac{1}{\Omega^2}-\frac{\alpha k_y}{k_\perp^2(\Omega+k_y\sigma)}=0, \tag{22}$$

where

$$\Omega=\frac{\omega-k_x v_{0i}}{\omega_0},\quad \omega_0\equiv\omega_{pi}\left(\frac{1+k_\perp^2\rho_e^2}{1+k_\perp^2\rho_e^2+\omega_{pe}^2/\omega_{Be}^2}\right)^{1/2},$$
$$\alpha=\frac{(\kappa_n-2\bar{\kappa}_B)\omega_0}{\omega_{Bi}(1+k_\perp^2\rho_e^2)},\quad \sigma=\frac{1}{\omega_0}\left[\frac{c}{B_0}\left(E_0+\frac{2T_e}{e}\bar{\kappa}_B\right)+\frac{k_x}{k_y}v_{0i}\right],$$
$$\bar{\kappa}_B=\frac{1+2k_\perp^2\rho_e^2}{1+k_\perp^2\rho_e^2}\cdot\kappa_B. \tag{23}$$

The instability studied belongs to the class of instabilities driven by the perpendicular current. The parameter σ is proportional to such a current. It consists of three parts—the electron $\mathbf{E}_0\times\mathbf{B}_0$ and magnetic drift flows and the ion flow parallel to the electric field—and characterizes the "drive" of gradient drift instability. The parameter α is responsible for plasma and magnetic field inhomogeneity.

Then, from Eq. (22), we obtain the following cubic equation for Ω with real coefficients

$$\Omega^3+\lambda\bar{\sigma}\Omega^2-\Omega-\bar{\sigma}=0, \tag{24}$$

where

$$\lambda=1-\frac{\alpha}{k_\perp^2\sigma},\quad \bar{\sigma}=k_y\sigma.$$

The parameter $\bar{\sigma}$ corresponds to the instability drive and, as it will be shown below, the parameter λ defines the necessary condition for gradient-drift instability.

The perturbations described by this equation are stable if and only if all its roots are real. Otherwise, there always exists an unstable solution with $\mathrm{Im}\,\Omega>0$. The condition under which all roots of cubic equation (24) are real can be written in the form

$$4\lambda^3\bar{\sigma}^4+(\lambda^2+18\lambda-27)\bar{\sigma}^2+4\geq 0. \tag{25}$$

First of all, we notice that for $\lambda=0$, the first term on the left hand side of inequality (25) disappears and stability condition takes the form

$$\bar{\sigma}^2\leq\frac{4}{27},\quad \text{if } \lambda=0. \tag{26}$$

Otherwise, on the left hand side of inequality (25), we have a quadratic trinomial with respect to $\bar{\sigma}^2$. Therefore, condition (25) can be rewritten in the form

$$\lambda^3(\bar{\sigma}^2-\mu_1)(\bar{\sigma}^2-\mu_2)\geq 0, \tag{27}$$

where $\mu_{1,2}$ are the roots of quadratic equation

$$4\lambda^3\mu^2+(\lambda^2+18\lambda-27)\mu+4=0. \tag{28}$$

These roots are described by the expressions

$$\mu_{1,2}=\frac{1}{8\lambda^3}\left[27-18\lambda-\lambda^2\mp\sqrt{(27-18\lambda-\lambda^2)^2-64\lambda^3}\right]. \tag{29}$$

The asymptotes of the roots are as follows (μ_1 corresponds to sign "–," μ_2 – to sign "+"):

$$\begin{aligned}&\mu_1\to-\frac{1}{4\lambda},\quad \mu_2\to-\frac{4}{\lambda^2}<0,\quad \text{when } \lambda\to-\infty;\\ &\mu_1\to\frac{4}{27},\quad \mu_2\to\frac{27}{4\lambda^3}\to\mp\infty,\quad \text{when } \lambda\to\mp 0;\\ &(\mu_1,\mu_2)\to 1,\quad \text{when } \lambda\to 1.\end{aligned}$$

Now we note that the determinant D of quadratic equation (28) [the expression under square root in Eq. (29)] can be represented in a very simple and compact form

$$D=(27-18\lambda-\lambda^2)^2-64\lambda^3\equiv(\lambda-1)(\lambda-9)^3.$$

It is clear that the roots μ_1 and μ_2 are real when $D>0$, i.e., when $\lambda\leq 1$ and $\lambda\geq 9$. At the same time, when $1<\lambda<9$, the roots are complex conjugates. Keeping this in mind, we carry out an analysis of stability of plasma perturbations.

(1) When $\lambda\geq 9$, both roots are real and negative because

$$\mu_1\cdot\mu_2=\frac{1}{\lambda^3}>0,\quad \mu_1+\mu_2=-(\lambda^2+18\lambda-27)/4\lambda^3<0,$$

so that $\mu_{1,2}=-|\mu_{1,2}|$. Then, condition (27) takes the form

$$\lambda^3\left(\bar{\sigma}^2+|\mu_1|\right)\left(\bar{\sigma}^2+|\mu_2|\right)\geq 0.$$

This condition is certainly satisfied for any $\bar{\sigma}$. Thus, in this range of λ, the perturbations are stable.

(2) When $1<\lambda<9$, the roots of Eq. (28) are complex conjugates and can be written in the form $\mu_1=A+iB$, $\mu_2=A-iB$. Then, condition (27) takes the form

$$\lambda^3\left[(\bar{\sigma}^2-A)^2+B^2\right]\geq 0.$$

This condition is certainly satisfied for any value of $\bar{\sigma}$, and therefore, when $1<\lambda<9$, the perturbations are stable.

(3) When $0<\lambda\leq 1$, both roots of Eq. (28) are real and positive because $(\mu_1\cdot\mu_2,\ \mu_1+\mu_2)>0$, and $\mu_1<\mu_2$. Since $\lambda>0$, stability condition (27) takes the form $\bar{\sigma}^2\leq\mu_1$, $\bar{\sigma}^2\geq\mu_2$. In terms of λ, these conditions can be written as

$$\begin{aligned}&\bar{\sigma}^2\leq\frac{1}{8\lambda^3}\left[27-18\lambda-\lambda^2-\sqrt{(1-\lambda)(9-\lambda)^3}\right],\\ &\bar{\sigma}^2\geq\frac{1}{8\lambda^3}\left[27-18\lambda-\lambda^2+\sqrt{(1-\lambda)(9-\lambda)^3}\right].\end{aligned} \tag{30}$$

Notice that for $\lambda\to 0$, the first inequality in Eq. (30) transforms into inequality (26).

(4) Finally, when $\lambda<0$, both roots are real and have different signs: μ_1 is positive, $\mu_1>0$, and μ_2 is negative, $\mu_2<0$. Then, it means that stability condition (27) takes the form $\bar{\sigma}^2\leq\mu_1$. In an explicit form, it is written as

$$\bar{\sigma}^2\leq-\frac{1}{8\lambda^3}\left[\sqrt{(1-\lambda)(9-\lambda)^3}+\lambda^2+18\lambda-27\right]. \tag{31}$$

It follows from the above analysis that a *sufficient* condition of stability of considered plasma perturbations is $\lambda\geq 1$. It takes place when $\alpha\sigma\leq 0$, i.e., if

$$\left(\frac{eE_0}{T_e}+\frac{1+2k_\perp^2\rho_e^2}{1+k_\perp^2\rho_e^2}\cdot\frac{d}{dx}\ln B_0^2+\frac{k_x}{k_y}\frac{\omega_{Bi}}{c_s}\frac{v_{0i}}{c_s}\right)\times\left\{\frac{d}{dx}\ln n_0-\frac{1+2k_\perp^2\rho_e^2}{1+k_\perp^2\rho_e^2}\cdot\frac{d}{dx}\ln B_0^2\right\}\leq 0. \tag{32}$$

We emphasize that this condition guaranties that both long-wavelength, lower-frequency and short-wavelength, higher-frequency (of order ω_0) perturbations are stable. For almost azimuthal perturbations with $k_x\ll k_y$ and negligible inhomogeneity of the magnetic field strength, this condition takes the form $\mathbf{E}_0\cdot\nabla n_0\leq 0$ which is complementary to the Simon-Hoh (S-H) instability condition.[32,33] Note that according to this criterion, the equilibria with the ballistic ion acceleration, described by Eq. (15), are always stable. Neglecting the FLR effects and equilibrium ion velocity in Eq. (32), one can easily obtain the generalized S-H stability criterion for the inhomogeneous magnetic field: $(V_{0E}+V_D)(\kappa_n-2\kappa_B)\geq 0$.

In the long-wavelength region, the perturbations are unstable if the inequality opposite to (31) is fulfilled. The long-wavelength perturbations previously studied in Refs. 20 and 21 correspond to $k_\perp^2\ll(\rho_e^{-2},l_0^{-2})$, where

$$l_0^2\equiv\frac{\omega_{Bi}}{\omega_{pi}^2(\kappa_n-2\kappa_B)}\cdot\left[\frac{c}{B_0}\left(E_0+2\frac{T_e}{e}\kappa_B\right)+\frac{k_x}{k_y}v_{0i}\right].$$

In this case, $\mu_1\to-1/4\lambda$ and the instability takes place if

$$\frac{1}{\omega_{Bi}}\left(\frac{cE_0}{B_0}+\frac{2cT_e}{eB_0}\kappa_B+\frac{k_x}{k_y}v_{0i}\right)\frac{d}{dx}\ln\left(\frac{n_0}{B_0^2}\right)>\frac{k_\perp^2}{4k_y^2}. \tag{33}$$

This instability condition for long-wavelength gradient drift perturbations is previously derived in Ref. 20.

According to the above analysis, the *necessary and sufficient condition* of gradient drift instability can be formulated as

$$\begin{cases}\bar{\sigma}^2>\mu_1, & \text{for } \lambda\leq 0;\\ \mu_1<\bar{\sigma}^2<\mu_2, & \text{for } 0<\lambda<1.\end{cases} \tag{34}$$

The full picture of instability is summarized in Fig. 1. The boundaries of the instability region are described by the curves $\bar{\sigma}^2=\mu_{1,2}$—see Eq. (29). At $\lambda\leq 0$, the instability region is located above the curve $\bar{\sigma}^2=\mu_1$ and at $0<\lambda<1$—between the curves $\bar{\sigma}^2=\mu_1$ and $\bar{\sigma}^2=\mu_2$ which intersect at the point $\lambda=1$. The region with $\lambda\geq 1$ is stable.

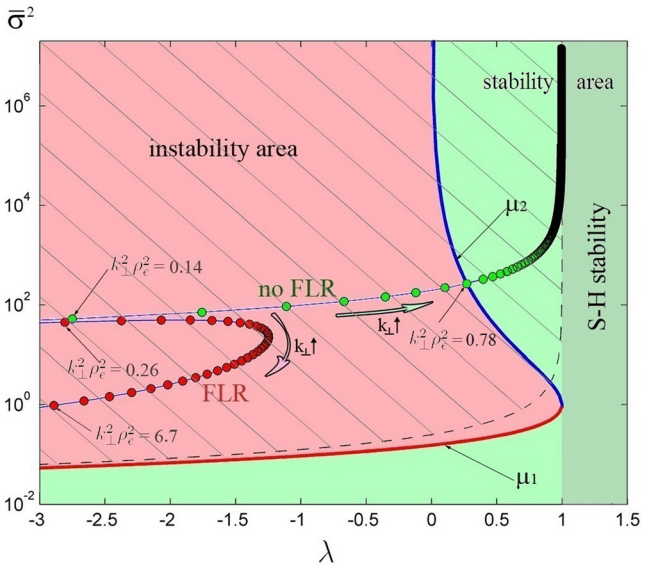

FIG. 1. Stability diagram in the plane $\bar{\sigma}^2$–λ. The dashed curve shows the stability boundary with no account of electron inertia; the corresponding instability region is dashed.

Now let us examine the role of the inertia and FLR effects, which can be understood from the above diagram. We neglect the equilibrium ion velocity, since typically in the experiments $v_{0i} \ll (V_{0E}, V_D)$ (the equilibrium ion velocity effects can be important for predominantly axial perturbations with $k_x \gg k_y$, which are not the particular case of this paper). First, we drop the inertia effect, setting $k_\perp^2\rho_e^2 \to 0$. In this limiting case, the parameters α and σ do not depend on the wavenumber, $\alpha_0 = \alpha|_{k_\perp^2\rho_e^2\to 0}$, $\sigma_0 = \sigma|_{k_\perp^2\rho_e^2\to 0}$ and are the functions of plasma parameters only. In terms of λ and $\bar{\sigma}$, dispersion relation (20) without the inertia effects takes the form

$$\bar{\sigma}(1-\lambda)\Omega^2 + \Omega + \bar{\sigma} = 0.$$

The stability boundary for this dispersion relation is given by the dependence $\bar{\sigma}^2 = 1/4(1-\lambda)$ [condition (33)] shown in Fig. 1 with the dashed line. The instability region is above this curve. Comparing the instability regions with and without the electron inertia effect, one can easily see that the inertia effect leads to the extension of the stability region for large values of instability drive $\bar{\sigma}$ ($\bar{\sigma}^2 > \bar{\sigma}_{\text{int}}^2$) and extra destabilization for small $\bar{\sigma}$ ($\bar{\sigma}^2 < \bar{\sigma}_{\text{int}}^2$), where $\bar{\sigma}_{\text{int}}^2 = 1/2\left(5\sqrt{5} - 11\right)$ corresponds to the intersection point of the curves $\bar{\sigma}^2 = \mu_2$ (upper stability boundary with the inertia effects) and $\bar{\sigma}^2 = 1/4(1-\lambda)$ (stability boundary with no inertia).

Now, let us fix the equilibrium parameters α_0 and σ_0 and follow the parametric curve $\bar{\sigma}^2(\lambda)$ defined by the wavenumber $k_\perp$ on the stability diagram. For strictly azimuthal modes ($k_x = 0$) and without taking into account the FLR effects, the curve is described by the relation $\bar{\sigma}^2 = \alpha_0\sigma_0/(1-\lambda)$ repeating the behavior of the stability boundary without electron inertia, $\bar{\sigma}^2 = 1/4(1-\lambda)$. As an example, in Fig. 1, the corresponding curve for $\alpha_0 = -488.42$ cm^{-1} and $\sigma_0 = -0.4024$ cm is shown with the black line with green circles (no FLR): $k_\perp$ grows along the curve (from the left to the right). These values of α_0 and σ_0 correspond to the following plasma parameters: $B_0 = 200$ G, $V_{0E} = 6\times 10^6$ cm/s, $n_0 = 0.5\times 10^{12}$ cm^{-3}, $T_e = 3.125$ eV, $\kappa_n = 1$ cm^{-1}, $\kappa_B = 1$ cm^{-1} and xenon atoms; these parameters are specific to dense partially magnetized plasmas typical for Hall plasma thrusters and magnetron discharges. Thus, without electron inertia effects, the whole spectrum of perturbations $k_\perp \in (0,\infty)$ is unstable at $\alpha_0\sigma_0 > 1/4$; at $\alpha_0\sigma_0 < 1/4$, all modes are stable. When we take into account the inertia effects, the cut-off of the short-wavelength modes occurs with the maximal possible $k_{\perp max}$ defined by the relation $\alpha_0\sigma_0/(1-\lambda) = \mu_2$, at the intersection with the μ_2 instability boundary in Fig. 1.

The contour-plots of frequencies and growth rates of unstable modes in the plane $\bar{\sigma}^2 - \lambda$ calculated from Eq. (24) with using the trigonometric Vieta's formula are shown in Fig. 2. Following the black line with green circles in Fig. 2(a), one can easily observe the growth of the frequency with the increase of $k_\perp$—from low-frequency, $\omega \ll \omega_{lh}$, to high-frequency, $\omega \gtrsim \omega_{lh}$. The high-frequency short-wavelength oscillations have larger growth rates than the low-frequency long-wavelength ones—see Fig. 2(b). At large values of σ_0 (strong drive), the maximal growth rate corresponds to $\lambda = 0$.

This condition uniquely defines the wavelength of the most unstable mode, $k_\perp^2|_{\lambda=0} = \alpha_0/\sigma_0$ (note that according to the necessary condition of instability (32), α_0 and σ_0 are always of the same sign in the instability region)

$$k_\perp|_{\lambda=0} = \frac{\omega_{lh}}{\rho_e\sqrt{\omega_{Be}\omega_{Bi}}}\sqrt{\frac{V_{*e}-V_D}{V_{0E}+V_D}}.$$

The stronger the drive, the longer the wavelength of the mode with the maximal growth rate. Since at large $\bar{\sigma}^2$ the instability threshold is defined by the point of intersection with the upper instability boundary μ_2 near $\lambda = 0$, in the model without FLR effects, the wavelength of the most unstable mode is close to the minimal admitted wavelength of unstable perturbations (maximal $k_\perp$ in the instability region).

The frequency of unstable modes near the upper instability boundary is of the order of ω_{lh} and higher—see Fig. 2(a). Thus, without FLR effects, the maximal growth rate have the high-frequency, long-wavelength perturbations [since $k_\perp|_{\lambda=0} \sim (\alpha_0/\sigma_0)^{1/2}$].

The FLR effects make the picture much more complex, since the parameters α and σ not only depend on the equilibrium plasma state but are also functions of $k_\perp$. As a result, at fixed plasma parameters, the function $\bar{\sigma}^2(\lambda)$ is not necessarily an increasing monotonic function—see black line with red circles (FLR) in Fig. 1, which is calculated for the same plasma parameters as above but takes into account the electron FLR effects, $k_\perp\rho_e \neq 0$. In the considered case, the FLR effects totally change the behavior of $\bar{\sigma}^2(\lambda)$: from strictly monotonic it becomes a multiple-valued function (note: dependence that the presented is not universal and is shown just as an example).

In the instability region for $k_\perp$ exceeding some value, both $\bar{\sigma}^2$ and λ become decreasing functions of $k_\perp$, thereby cutting-off the curve from the region corresponding to high-frequency oscillations. A complete stabilization of the short-wavelength modes takes place when the curve $\bar{\sigma}^2(\lambda)$ intersects the lower instability boundary, μ_1 (in Fig. 2, the point of this intersection is shown in a separate window).

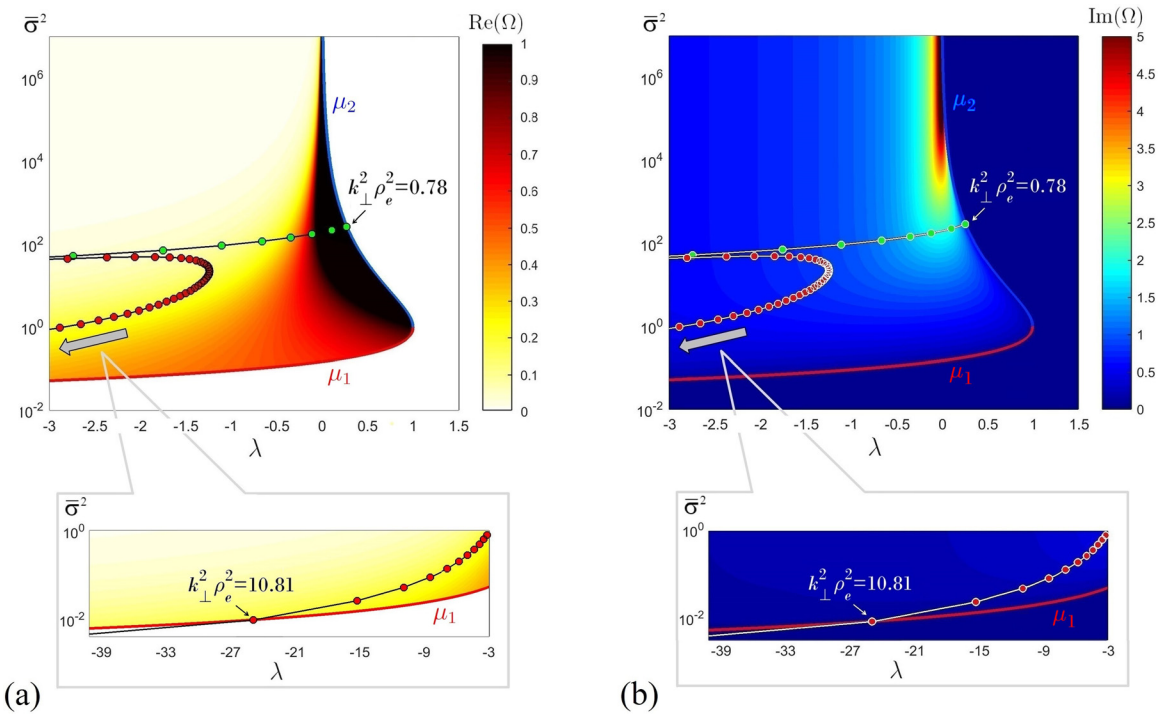

FIG. 2. Contour-plots of frequencies (a) and growth rates (b) of unstable modes in the plane $\bar{\sigma}^2 - \lambda$. In (a), the region of stable perturbation is shown in white and the unstable modes with $\omega > \omega_{lh}$ are shown in black.

The relative contribution of the inertia effects and the electron FLR effects depends on the ratio between the scale length $(\sigma_0/\alpha_0)^{1/2}$ at which the inertia effects become important and the electron Larmor radius ρ_e or, in other words, on the dimensionless parameter $\Delta \equiv \alpha_0\rho_e^2/\sigma_0$.

For weak instability drive (defined by the parameter σ_0) such that $\Delta \gg 1$, the instability is stabilized by the electron FLR effects before the inertia effects become important. The dependencies of the frequencies and the growth rates of unstable perturbations for such a case with $\sigma_0 = -0.12$ cm corresponding to $V_{0E} = 3.4 \times 10^6$ cm/s are presented in Fig. 3(a). The other plasma parameters are taken as before ($B_0 = 200$ G, $n_0 = 0.5 \times 10^{12}$ cm^{-3}, $T_e = 3.125$ eV, $\kappa_n = 1$ cm^{-1}, $\kappa_B = 1$ cm^{-1}, xenon) so that $\alpha_0 = -488.4$ cm^{-1}, and $\Delta \simeq 5.64$. One can clearly see a significant difference between the curves calculated with the FLR effects and without FLR effects. The FLR effects stabilize the instability at $k_\perp\rho_e \lesssim 0.3$ and only relatively low-frequency perturbations with $\omega \leq 0.02\omega_{lh}$ are unstable. The omission of the FLR effects results in the instability at higher $k_\perp$ (up to $k_\perp\rho_e \lesssim 3.35$). The frequencies of the unstable smaller-wavelength perturbations are also higher (up to $\omega \simeq 2.5\,\omega_{lh}$). It is clear that the model that does not take into account the FLR effects is not applicable for such plasma parameters.

In the opposite case of strong instability drive $\sigma_0 = -3.76$ cm corresponding to $V_{0E} = 3 \times 10^7$ cm/s, we have $\Delta \simeq 0.06$. In this case, the stabilization of instability by the electron inertia effects takes place for the perturbations with the wavelengths that are larger than the electron Larmor radius (at $k_\perp\rho_e \simeq 0.25$). Therefore, the FLR effects only slightly influence the instability region, the frequencies, and the growth rates of the unstable perturbations [see Fig. 3(b)].

Finally, in the intermediate case for the parameters used before in Fig. 2 ($\sigma_0 = -0.40$ cm, $V_{0E} = 6 \times 10^6$ cm/s), we have $\Delta \simeq 0.54$ so that the inertia effects and the FLR effects become important at the same wavelengths. The interaction of these two effects essentially changes the results [see Fig. 3(c)]. The instability region extends up to shorter wavelengths (up to $k_\perp\rho_e \simeq 3.3$) compared to the model without FLR effects. Also, one can see a sufficient reduction of the frequency and the growth rate of unstable modes at $0.4 \lesssim k_\perp\rho_e \lesssim 0.75$. It means that the model without FLR effects becomes inapplicable for the perturbations with $k_\perp\rho_e \gtrsim 0.4$.

Here, we have demonstrated the influence of the electron FLR on gradient drift instability on several practical examples. In the general case, gradient drift instability with finite electron FLR effects becomes a complex multiparameter problem and requires more analysis. A detailed treatment of the general case for azimuthal perturbations with $k_x \ll k_y$ is presented in the separate paper.[34]

V. CONCLUSION

In this paper, we have developed the generalized fluid model for the gradient drift instabilities of partially magnetized plasmas in the frequency range $\omega_{Bi} \ll \omega \ll \omega_{Be}$ driven by the equilibrium current perpendicular to the magnetic field. The model takes into account the electron inertia, gradients of plasma density and magnetic field, and effects of the finite electron temperature—the electron diamagnetic drift and FLR effects. The electron FLR effects in the inhomogeneous external magnetic field are considered by taking into account the collisionless electron gyroviscosity. Our generalized model exactly describes the electron dynamics for the long-wavelength motions with

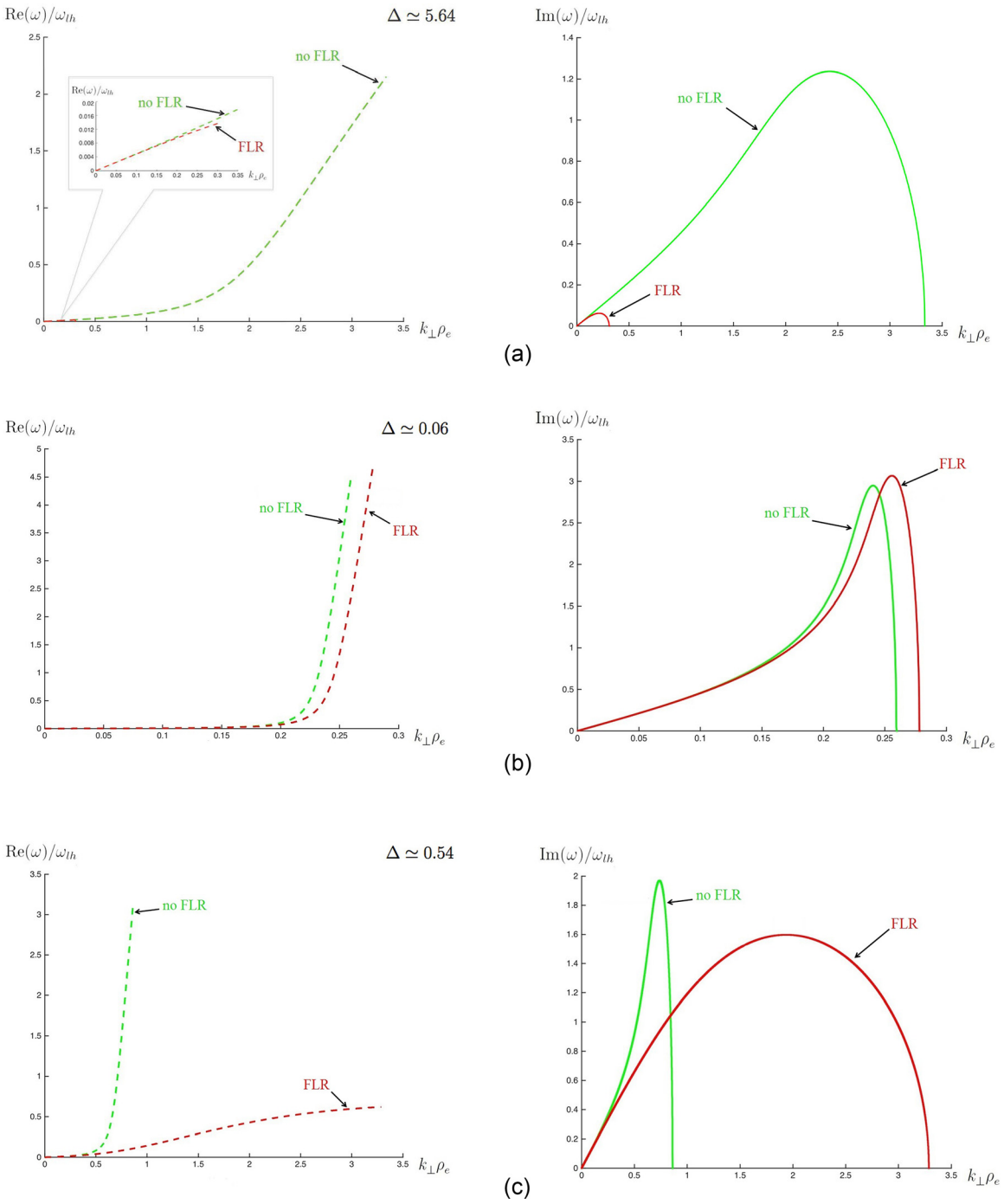

FIG. 3. The dependencies of frequencies (left column) and growth rates (right column) of unstable modes on $k_\perp$ for different V_{0E}: (a) $V_{0E} = 3.4 \times 10^6$ cm/s; (b) $V_{0E} = 3 \times 10^7$ cm/s; (c) $V_{0E} = 6 \times 10^6$ cm/s. Here $B_0 = 200$ G, $n_0 = 0.5 \times 10^{12}$ cm^{-3}, $T_e = 3.125$ eV, $\kappa_n = 1$ cm^{-1}, $\kappa_B = 1$ cm^{-1}, and xenon atoms are considered.

$k_\perp \rho_e \ll 1$ and qualitatively correctly—in the sense of Padé approximants—for the short-wavelength modes with $k_\perp \rho_e \simeq 1$ and higher (up to $k_\perp \rho_e \gg 1$).

We have derived a dispersion relation that generalizes earlier known dispersion relations of Refs. 1, 12–14, 17, and 20. In addition to the dispersion relations of Refs. 1, 12–14, and 17, it takes into account the electron temperature effects (electron magnetic drift and FLR effects) and in addition to the dispersion relation of Ref. 20—the electron inertia and FLR effects. Our model for the first time includes the effects of the magnetic field gradient in the higher order FLR terms.

On the basis of dispersion relation (19), the stability properties of electrostatic oscillations are studied. The sufficient condition of stability (32) is analytically obtained. Also, the necessary and sufficient condition for gradient drift instability in terms of the plasma equilibrium parameters and the wavenumber of oscillations is formulated [see Eq. (34)].

It is shown that the electron inertia stabilizes the short-wavelength perturbations setting the upper limits for the

growth rate and for the wave-number of unstable modes. Near the instability threshold, the FLR effects can stabilize high-frequency short-wavelength modes so that only the long-wavelength oscillations remain unstable.

The detailed stability analysis of azimuthal modes with electron FLR effects is presented in Ref. 34 where the gradient drift instability is studied for the plasma equilibrium with the negligibly weak electric field $|eE_0/(\kappa_B T_e)| \ll 1$ and for the general case of the moderate or strong electric field, $|eE_0/(\kappa_B T_e)| \gtrsim 1$.

ACKNOWLEDGMENTS

This work was supported in part by the Russian Science Foundation (Project No. 17-12-01470). V.I.I. appreciates the financial support of the Ministry of Education and Science of the Russian Federation (Agreement Nos. 02.A03.21.0008 and 3.2223.2017).

[1]A. B. Mikhailovskii, *Theory of Plasma Instabilities: Volume 2: Instabilities of an Inhomogeneous Plasma* (Consultants Bureau, New York, 1974), Vol. 2.
[2]A. B. Mikhailovskii, *Electromagnetic Instabilities in an Inhomogeneous Plasma* (Taylor and Francis, 1992).
[3]J.-P. Boeuf, Front. Phys. Plasmas. Phys. **2**, 74 (2014).
[4]A. I. Morozov and V. V. Savelyev, in *Reviews of Plasma Physics*, edited by B. B. Kadomtsev and V. D. Shafranov (Consultants Bureau, New York, 2000), Vol. 21, pp. 203–391.
[5]V. P. Pastukhov, Sov. J. Plasma Phys. **6**, 549 (1980).
[6]V. V. Piterskii, V. P. Pastukhov, M. S. Ioffe, B. I. Kanaev, and E. E. Yushmanov, Sov. J. Plasma Phys. **14**, 94 (1988).
[7]M. S. Ioffe, B. I. Kanaev, V. P. Pastukhov, V. V. Piterskii, and E. E. Yushmanov, Plasma Phys. Rep. **20**, 405 (1994).
[8]R. C. Davidson and N. A. Krall, Nucl. Fusion **17**, 1313 (1977).
[9]A. M. Fridman, Sov. Phys. Dokl. **9**, 75 (1964).
[10]A. I. Smolyakov, O. Chapurin, W. Frias, O. Koshkarov, I. Romadanov, T. Tang, M. Umansky, Y. Raitses, I. D. Kaganovich, and V. P. Lakhin, Plasma Phys. Controlled Fusion **59**, 014041 (2017).
[11]V. I. Ilgisonis and V. P. Pastukhov, "Transversal electron losses in magneto-electrostatic traps with low pressure of plasma," preprint IAE-3495/6. Moscow: I.V. Kurchatov Institute of Atomic Energy, 1981.
[12]A. B. Mikhailovskii and V. S. Tsypin, Sov. Phys. JETP Lett. **3**, 158 (1966).
[13]A. I. Morozov, Yu. V. Esipchuk, A. M. Kapulkin, V. A. Nevrovskii, and V. A. Smirnov, Sov. Phys. Tech. Phys. **17**, 482 (1972).
[14]Yu. V. Esipchuk and G. N. Tilinin, Sov. Phys. Tech. Phys. **21**, 417 (1976).
[15]D. Tomilin, Phys. Plasmas **20**, 042103 (2013).
[16]V. D. Nikitin, D. Tomilin, A. Lovtsov, and A. Tarasov, Europhys. Lett. **117**, 45001 (2017).
[17]E. Y. Choueiri, Phys. Plasmas **8**, 1411 (2001).
[18]E. Chesta, C. Lam, N. Meezan, D. Schmidt, and M. Cappelli, IEEE Trans. Plasma Sci. **29**, 582 (2001).
[19]A. Kapulkin and M. M. Guelman, IEEE Trans. Plasma Sci. **36**, 2082 (2008).
[20]W. Frias, A. I. Smolyakov, I. D. Kaganovich, and Y. Raitses, Phys. Plasmas **19**, 072112 (2012).
[21]W. Frias, A. I. Smolyakov, I. D. Kaganovich, and Y. Raitses, Phys. Plasmas **20**, 052108 (2013).
[22]N. A. Krall and P. C. Liewer, Phys. Rev. A **4**, 2094 (1971).
[23]R. C. Davidson and N. T. Gladd, Phys. Fluids **18**, 1327 (1975).
[24]J. D. Huba and C. S. Wu, Phys. Fluids **19**, 988 (1976).
[25]N. A. Krall and J. B. McBride, Phys. Fluids **19**, 1970 (1976).
[26]A. Fruchtman, Phys. Fluids B **1**, 422 (1989).
[27]D. Escobar and E. Ahedo, Phys. Plasmas **21**, 043505 (2014).
[28]D. Escobar and E. Ahedo, Phys. Plasmas **22**, 102114 (2015).
[29]A. B. Mikhailovskii and V. S. Tsypin, Beitr. Plasmaphys. **24**, 335 (1984).
[30]J. J. Ramos, Phys. Plasmas **12**, 112301 (2005).
[31]T. J. Schep, B. N. Kuvshinov, and F. Pegoraro, Phys. Plasmas **1**, 2843 (1994).
[32]A. Simon, Phys. Fluids **6**, 382 (1963).
[33]F. C. Hoh, Phys. Fluids **6**, 1184 (1963).
[34]V. P. Lakhin, V. I. Ilgisonis, A. I. Smolyakov, E. A. Sorokina, and N. A. Marusov, Phys. Plasmas **25**, 012107 (2018).